A mathematical framework for modeling propagation of infectious diseases with mobile individuals

A mathematical framework for modeling propagation of infectious diseases with mobile individuals

Corrado Possieri and Alessandro Rizzo

***Abstract*— In this paper, we propose a novel framework for modeling the diffusion of infectious diseases. In particular, we show that the infectious spread occurring between individuals that are capable of moving along a (possibly stochastic) digraph can be modeled through a (generally larger, yet sparser) stochastic digraph. The use of the proposed modeling framework makes available the whole spectrum of computational tools for stochastic digraphs, toward the quantitative study of epidemic spreading on complex networks. Salient examples are provided throughout the paper.**

I. Introduction

Mathematical models are of paramount importance for the analysis of the propagation of infectious diseases, to assess the validity of conjectures, perform what-if analyses, design pharmaceutical or non-pharmaceutical interventions, sensitivity analyses, and extract key information from data [1], [2]. For instance, in [3], the evolution of the epidemic states is described by a Markov process; in [1], [4], the dynamics of the total number of healthy and infected individuals is described through population dynamics [5]; in [6], a moment closure method is proposed to efficiently propagate infection statistics; in [7], [8], deterministic dynamical models, in which the state represent the fractions of infected and susceptible individuals, have been proposed to model the spread of infectious diseases in large populations; in [9], [10], [11], [12], stochastic model over (static) networks have been proposed to model the interactions among individuals; in [13], [14], [15], [16], discrete-time activity driven networks have been proposed to study epidemic spreading over networks; and, in [17], weighted and directed time-varying graph structures are employed to model the spread of an infectious disease.

The main objective of this paper is to propose a novel framework for modeling the epidemic diffusion of infectious diseases in populations of mobile agents [18]. The interest in this class of models relies on the fact that they allow to consider the spread of infectious diseases due to migrating populations, which is one of the crucial aspects to be taken into account in modern word [19], [20], [21], where migration has become a phenomenon of great importance [22].

In particular, we show that stochastic digraphs can be efficiently used to represent the dynamics of propagation of infectious diseases with mobile agents. The key advantage of using this mathematical framework is that several tools available in the literature, such as those in [23], [24], can be readily employed to characterize the properties of stochastic digraphs, thus allowing to perform quantitative analysis without resorting to extensive numerical simulations.

C. Possieri and A. Rizzo are with Dipartimento di Elettronica e Telecomunicazioni, Politecnico di Torino, 10129 Torino, Italy.

Emails: corrado.possieri@polito.it, alessandro.rizzo@polito.it

II. Stochastic digraphs

Let $\mathbb{Z}_n := \{0, \dots, n-1\}$. Given $\mathcal{I} \subset \mathbb{Z}_n$, the *indicator function on* $\mathcal{I}$ is defined as

$$\mathbb{I}_{\mathcal{I}}(\zeta) := \begin{cases} 1, & \text{if } \zeta \in \mathcal{I}, \\ 0, & \text{otherwise.} \end{cases}$$

The symbol $\mathbb{E}[\cdot]$ denotes the expected value.

A directed graph (*digraph*) is a pair $\mathcal{G} := (\mathcal{V}, \mathcal{E})$, where $\mathcal{V} = \mathbb{Z}_n$ is the node set and $\mathcal{E} \subset \mathbb{Z}_n \times \mathbb{Z}_n$ is the (ordered) edge set [25], [26]. In $\mathcal{G} = (\mathcal{V}, \mathcal{E})$, the *out–neighborhood of* a is $\mathcal{N}^o(a) := \{b \in \mathbb{Z}_n : (a, b) \in \mathcal{E}\}$.

A *stochastic directed graph* (or, shortly, *stochastic digraph*) is a triple $\boldsymbol{\mathcal{G}} = (\mathcal{V}, \boldsymbol{\mathcal{E}}, \mu(\cdot))$, where

- $\mathcal{V} = \mathbb{Z}_n$ is the node set;
- $\boldsymbol{\mathcal{E}} := \{\boldsymbol{\mathcal{E}}_s\}_{s=0}^{r-1}$, with r being an integer, is a sequence of edge sets $\boldsymbol{\mathcal{E}}_s$ such that $\mathcal{G}_s := (\mathcal{V}, \boldsymbol{\mathcal{E}}_s)$ is a digraph, $s \in \mathbb{Z}_r$. Here, we can consider r as a finite integer, as the number of edge sets $\mathcal{E}$ such that $(\mathcal{V}, \mathcal{E})$ is a graph is finite [24]);
- $\mu(\cdot)$ is a distribution function derived from an infinite sequence of independent, identically distributed (i.i.d.) random variables $\boldsymbol{w}_k : \Omega \to \mathbb{Z}_r$ $k \geqslant 0$, defined on the probability space $(\Omega, \mathcal{F}, \mathbb{P})$, $\mu : \mathbb{Z}_r \to [0, 1]$,

$$\mu(s) = \mathbb{P}(\omega \in \Omega : \boldsymbol{w}_k(\omega) = s).$$

Define the set–valued map $H : \mathbb{Z}_n \times \mathbb{Z}_r \rightrightarrows \mathbb{Z}_n$,

$$H(a, w) := \{b \in \mathbb{Z}_n : (a, b) \in \boldsymbol{\mathcal{E}}_s\}; \tag{1}$$

for each $s \in \mathbb{Z}_r$, which maps each $a \in \mathbb{Z}_n$ in the out–neighborhood $\mathcal{N}_w^o(a)$ of a in $\mathcal{G}_s := (\mathcal{V}, \boldsymbol{\mathcal{E}}_s)$, $s \in \mathbb{Z}_r$. Thus, following [23], the stochastic digraph $\boldsymbol{\mathcal{G}} = (\mathcal{V}, \boldsymbol{\mathcal{E}}, \mu(\cdot))$ can be equivalently represented as

$$a^+ \in H(a, w).$$

A sequence $(\boldsymbol{\phi}, \boldsymbol{z}) := \{(\boldsymbol{\phi}_k, \boldsymbol{z}_k)\}_{k=0}^{K}$ is a *regular directed path of length* K *of* $\boldsymbol{\mathcal{G}} := (\mathcal{V}, \boldsymbol{\mathcal{E}}, \mu(\cdot))$ *starting at* x if

- $\boldsymbol{\phi}_0 = x$;
- $\boldsymbol{\phi}_{k+1} \in \mathcal{N}_{\boldsymbol{z}_k}^o(\boldsymbol{\phi}_k)$, for all $k \in \{0, \dots, K-1\}$.

A map $\boldsymbol{a}$ from Ω to sequences in $\mathbb{Z}_n$ is a *stochastic directed path from* a, denoted $\boldsymbol{a} \in \mathcal{S}_r(a)$, if

- **Pathwise feasibility:** for each $\omega \in \Omega$, the sequence $\{(\boldsymbol{a}_k(\omega), \boldsymbol{w}_k(\omega))\}_{k=0}^{\boldsymbol{K}(\omega)}$ is a regular directed path from a, where $\boldsymbol{K} : \Omega \to \mathbb{Z}_{\geqslant 0} \cup \{\infty\}$ is the path length.

- **Causal measurability:** for each $k \in \mathbb{Z}_{\geqslant 0}$, the mapping $\omega \mapsto \boldsymbol{a}_{k+1}(\omega)$ is $\mathcal{F}_k$–measurable, where $(\mathcal{F}_0, \mathcal{F}_1, \mathcal{F}_2, \dots)$ is the minimal filtration of $\boldsymbol{w}$.

By [23], the set-valued mapping $H(a, w)$ defined in (1) satisfies the standing assumption of [27], [28], [29], and hence stochastic directed paths exist and are well defined.

It is worth noticing that if $H(a, w)$ is a singleton (possibly, empty) for all $(a, w) \in \mathbb{Z}_n \times \mathbb{Z}_r$, then the transition probabilities in the corresponding stochastic digraph can be represented through a Markov chain. In particular, the (i, j)-th entry of the transition matrix of such a Markov chain is

$$p_{i,j} = \mathbb{P}(\boldsymbol{x}_{k+1} = j | \boldsymbol{x}_k = i) = \sum_{r \in \{\rho \in \mathbb{Z}_r : H(i,\rho) = j\}} \mu(r).$$

On the other hand, in general, i.e., when one allows $H(a, w)$ to be a set-valued map, stochastic digraphs have more general representation capabilities since they can represent stochastic processes having non-unique solutions (i.e., the set $\mathcal{S}_r(a)$ need not be a singleton for all $a \in \mathbb{Z}_n$).

III. Modeling of the propagation of infectious diseases with mobile agents

In this section, we show that it is possible to encode through a stochastic digraph the dynamics of the propagation of infectious diseases in populations of mobile agents. In particular, we consider three different classes of infectious diseases: the susceptible-infected (SI) model (Section III-A), in which infected individuals cannot recover from the infection, the susceptible-infected-susceptible (SIS) model (Section III-B), in which individuals recover from the infection, but are susceptible to being re-infected, and the susceptible-infected-recovered (SIR) model (Section III-C), in which individuals recover from the infection and are immunized (or dead) after one round of infection. Independently of the class of epidemics, we assume that individuals move over a stochastic digraph (thus allowing also deterministic motion) and that an individual may become infected if he/she shares the same position of another infected individual, according to a given stochastic rule.

The strategy that is used to find a stochastic digraph that models the propagation of the disease in populations of mobile agents is detailed as follows:

- map the overall state of all the individuals (i.e., the pair position of each individual – infectious state) to a nonnegative integer (coding the nodes of a larger stochastic digraph) through a bijective map;
- determine the stochastic state transitions between nodes of the stochastic digraph of the previous point; and
- compute the transition probabilities by taking into account the probability of infection/healing, according to the specific epidemic dynamics.

By using such an approach, we obtain a stochastic digraph in which each node is in one-to-one correspondence with a state of all the individuals (i.e., their position and their infectious state) and in which transitions between one state and another are governed by a stochastic process. In particular, as it is shown in the subsequent Theorems 1, 2, and 3, the stochastic digraph obtained by using this procedure fully represents the (stochastic) propagation dynamics of the infectious disease.

A. The SI model

The *SI model with mobile agents* is defined as follows:

(i) we consider a population of N individuals;

(ii) the state of the i-th individual is defined as $x^i = \begin{bmatrix} p^i & s^i \end{bmatrix}^\top$, where $p^i \in \mathbb{Z}_n$ denotes the discretized position of each agent and $s^i \in \mathbb{Z}_2$ denotes the health state of the individual: $p^i = 0$ if the i-th agent is *susceptible* or $p^i = 1$ if it is *infected*, $i = 1, \dots, N$;

(iii) the position of each agent is updated at each step according to a given stochastic digraph[1] $\boldsymbol{\mathcal{G}} = (\mathcal{V}, \boldsymbol{\mathcal{E}}, \mu(\cdot))$,

$$p^{i^+} \in H(p^i, v), \tag{2}$$

where $\boldsymbol{v}_k : \Omega \to \mathbb{Z}_r$, $k \in \mathbb{Z}_{\geqslant 0}$, is a sequence of i.i.d. random variables and H is defined as in (1);

(iv) each individual (say i) in susceptible status (i.e., $s^i = 0$) can transition to infected as follows: if there is another individual (say j) that is infected (i.e., $s^j = 1$) and that shares the same position (i.e., $p^i = p^j$), then the individual become infected with probability α;

Note that we are not constraining the number of admissible positions with respect to the number of agents (namely, $N < r$, $N = r$, and $N > r$ are all admissible cases in the considered scenario). The next theorem states that there exists a stochastic digraph $\boldsymbol{\mathcal{SI}}$ that, given the rules (i)–(iv), model the behavior of the SI dynamics with mobile agents.

Theorem 1. *Given the rules (i)–(iv), there exists a stochastic digraph $\boldsymbol{\mathcal{SI}}$ that models the SI dynamics with mobile agents.*

The following exemplifies the application of the technique supported by Theorem 1 for determining a stochastic digraph that models the SI dynamics with mobile agents.

Example 1. Let $N = 2$ and assume that each individual moves along the digraph depicted in Fig. 1.

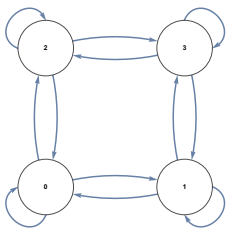

Fig. 1: Graph of the admissible movements of the 2 agents.

[1]Note that, in such a scenario, the graph describing the allowed movements of the individuals can also be a deterministic digraph, which corresponds to select $\boldsymbol{\mathcal{E}} = \mathcal{E}_0$ and $\mu(0) = 1$; see Example 1. In such a case, we are not constraining the motion of the individuals to have a predetermined probability structure, but we are considering all the possible motions that are compatible with the digraph.

By using Theorem 1, one obtains a stochastic digraph with $\boldsymbol{\mathcal{SI}} = (\bar{\mathcal{V}}, \bar{\boldsymbol{\mathcal{E}}}, \bar{\mu}(\cdot))$ with $\bar{\mathcal{V}} = \mathbb{Z}_{64}$, $\bar{r} = 4$, $\bar{\boldsymbol{\mathcal{E}}} = \{\bar{\mathcal{E}}_0, \bar{\mathcal{E}}_1, \bar{\mathcal{E}}_2, \bar{\mathcal{E}}_3\}$, $\mu(0) = (1-\alpha)^2$, $\mu(1) = \alpha(1-\alpha)$. $\mu(2) = \alpha(1-\alpha)$, and $\mu(3) = \alpha^2$, where the graphs $\mathcal{G}_i = (\bar{\mathcal{V}}, \mathcal{E}_i)$, $i = 0, \ldots, 3$, correspond to the adjacency matrices illustrated in Fig. 2. In particular, the adjacency matrix of $\mathcal{G}_i = (\bar{\mathcal{V}}, \mathcal{E}_i)$ is in $\{0,1\}^{\bar{n}\times\bar{n}}$ and its (j_1, j_2)th entry equals 1 (represented with a black box) if $(j_1, j_2) \in \mathcal{E}_i$, or equals 0 (represented with a white box) if $(j_1, j_2) \notin \mathcal{E}_i$, for $i = 1, \ldots, 4$.

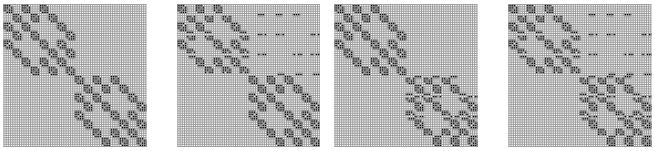

(a) $(1-\alpha)^2$. (b) $\alpha(1-\alpha)$. (c) $\alpha(1-\alpha)$. (d) α^2.

Fig. 2: Adjacency matrices of the graphs $\mathcal{G}_i$, $i = 0, \ldots, 3$. The matrix is black-and-white coded, where a black cell corresponds to a "1" entry, and a white case to a "0" entry.

B. The SIS model

The *SIS model with mobile agents* is defined as follows:

(I) we consider a population of N individuals;

(II) the state of the i-th individual is defined as $x^i = \begin{bmatrix} p^i & s^i \end{bmatrix}^\top$, where $p^i \in \mathbb{Z}_n$ denotes the discretized position of each agent and $s^i \in \mathbb{Z}_2$ denotes the health state of the individual: $p^i = 0$ if the i-th agent is *susceptible* or $p^i = 1$ if it is *infected*, $i = 1, \ldots, N$;

(III) the position of each agent is updated at each step according to a given stochastic digraph $\boldsymbol{\mathcal{G}} = (\mathcal{V}, \boldsymbol{\mathcal{E}}, \mu(\cdot))$,

$$p^{i^+} \in H(p^i, v), \tag{3}$$

where $\boldsymbol{v}_k : \Omega \to \mathbb{Z}_r$, $k \in \mathbb{Z}_{\geqslant 0}$, is a sequence of i.i.d. random variables;

(IV) each individual (say i) in susceptible status (i.e., $s^i = 0$) can transition to infected as follows: if there is another individual (say j) that is infected (i.e., $s_j = 1$) and that shares the same position (i.e., $p^i = p^j$), then the individual becomes infected with probability α;

(V) each infected individual can transition to susceptible status with probability β.

The following theorem states that there exists a stochastic digraph $\boldsymbol{\mathcal{SIS}}$ that, given the rules (I)–(V), models the behavior of the SIS dynamics with mobile agents.

Theorem 2. *Given the rules (I)–(V), there exists a stochastic digraph $\boldsymbol{\mathcal{SIS}}$ that models the SIS dynamics with mobile agents.*

The following exemplifies the application of the technique supported by Theorem 2 for determining a stochastic digraph that represents the SIS model with mobile agents.

Example 2. Let $N = 2$ and assume that each individual moves along the same digraph considered in Example 1 (namely, the one depicted in Fig. 1). By using the tools given in Theorem 2, one obtains a stochastic digraph with $\boldsymbol{\mathcal{SIS}} = (\bar{\mathcal{V}}, \bar{\boldsymbol{\mathcal{E}}}, \bar{\mu}(\cdot))$ with $\bar{\mathcal{V}} = \mathbb{Z}_{64}$, $\bar{r} = 16$, where the graphs $\mathcal{G}_i = (\bar{\mathcal{V}}, \bar{\mathcal{E}}_i)$, $i = 0, \ldots, 15$, correspond to the adjacency matrices illustrated in Fig. 3 (the same conventions employed in Fig. 2 have been used).

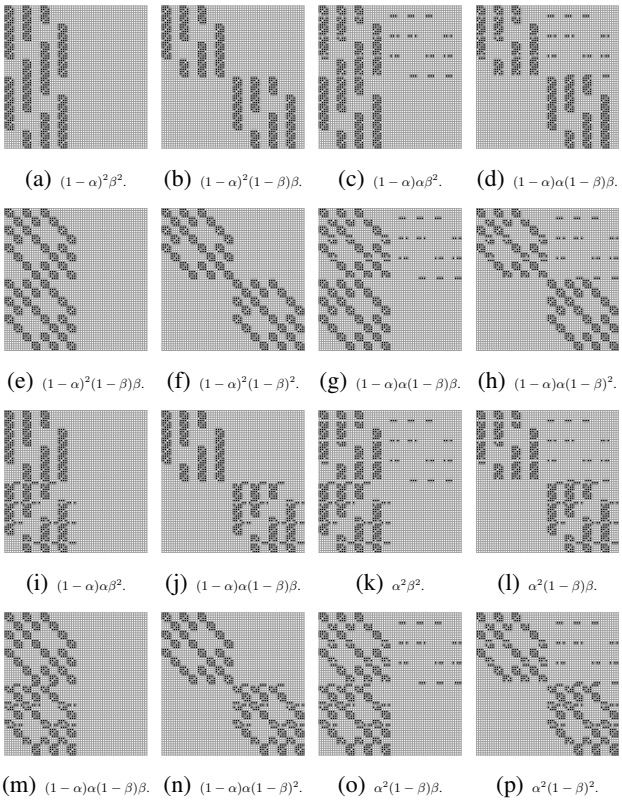

(a) $(1-\alpha)^2\beta^2$. (b) $(1-\alpha)^2(1-\beta)\beta$. (c) $(1-\alpha)\alpha\beta^2$. (d) $(1-\alpha)\alpha(1-\beta)\beta$.

(e) $(1-\alpha)^2(1-\beta)\beta$. (f) $(1-\alpha)^2(1-\beta)^2$. (g) $(1-\alpha)\alpha(1-\beta)\beta$. (h) $(1-\alpha)\alpha(1-\beta)^2$.

(i) $(1-\alpha)\alpha\beta^2$. (j) $(1-\alpha)\alpha(1-\beta)\beta$. (k) $\alpha^2\beta^2$. (l) $\alpha^2(1-\beta)\beta$.

(m) $(1-\alpha)\alpha(1-\beta)\beta$. (n) $(1-\alpha)\alpha(1-\beta)^2$. (o) $\alpha^2(1-\beta)\beta$. (p) $\alpha^2(1-\beta)^2$.

Fig. 3: Adjacency matrices of the graphs $\mathcal{G}_i$, and corresponding values of $\mu(i)$, $i = 0, \ldots, 15$.

C. The SIR model

The *SIR model with mobile agents* is defined as follows:

(a) we consider a population of N individuals;

(b) the state of the i-th individual is defined as $x^i = \begin{bmatrix} p^i & s^i \end{bmatrix}^\top$, where $p^i \in \mathbb{Z}_n$ denotes the discretized position of each agent and $s^i \in \mathbb{Z}_3$ denotes the health state of the i-th agent: $p^i = 0$ if it is *susceptible*, $p^i = 1$ if it is *infected*, or $p^i = 2$ if it is *recovered*, $i = 1, \ldots, N$;

(c) the position of each agent is updated at each step according to a given stochastic digraph $\boldsymbol{\mathcal{G}} = (\mathcal{V}, \boldsymbol{\mathcal{E}}, \mu(\cdot))$,

$$p^{i^+} \in H(p^i, v), \tag{4}$$

where $\boldsymbol{v}_k : \Omega \to \mathbb{Z}_r$, $k \in \mathbb{Z}_{\geqslant 0}$, is a sequence of i.i.d. random variables;

(d) each individual (say i) in susceptible status (i.e., $s^i = 0$) can transition to infected as follows: if there is another individual (say j) that is infected (i.e., $s_j = 1$) and that shares the same position (i.e., $p^i = p^j$), then the individual becomes infected with probability α;

(e) each infected individual can transition to recovered status with probability γ.

The following theorem states that there exists a stochastic digraph $\boldsymbol{\mathcal{SIR}}$ that, given the rules (a)–(e), models the behavior of the SIR dynamics with mobile agents.

Theorem 3. *Given the rules (a)–(e), there exists a stochastic digraph $\boldsymbol{\mathcal{SIR}}$ that models the SIR dynamics with mobile agents.*

The following exemplifies the application of the technique supported by Theorem 3 for determining a stochastic digraph that models the SIR dynamics with mobile agents.

Example 3. Let $N = 2$ and assume that each individual moves along the same digraph considered in Examples 1 and 2 (namely, the one depicted in Fig. 1). By using the tools given in Theorem 3, one obtains a stochastic digraph with $\boldsymbol{\mathcal{SIR}} = (\bar{\mathcal{V}}, \bar{\boldsymbol{\mathcal{E}}}, \bar{\mu}(\cdot))$ with $\bar{\mathcal{V}} = \mathbb{Z}_{144}$, $\bar{r} = 16$, where the graphs $\mathcal{G}_i = (\bar{\mathcal{V}}, \bar{\mathcal{E}}_i)$, $i = 0, \ldots, 15$, correspond to the adjacency matrices illustrated in Fig. 4 (the same conventions employed in Fig. 2 have been used).

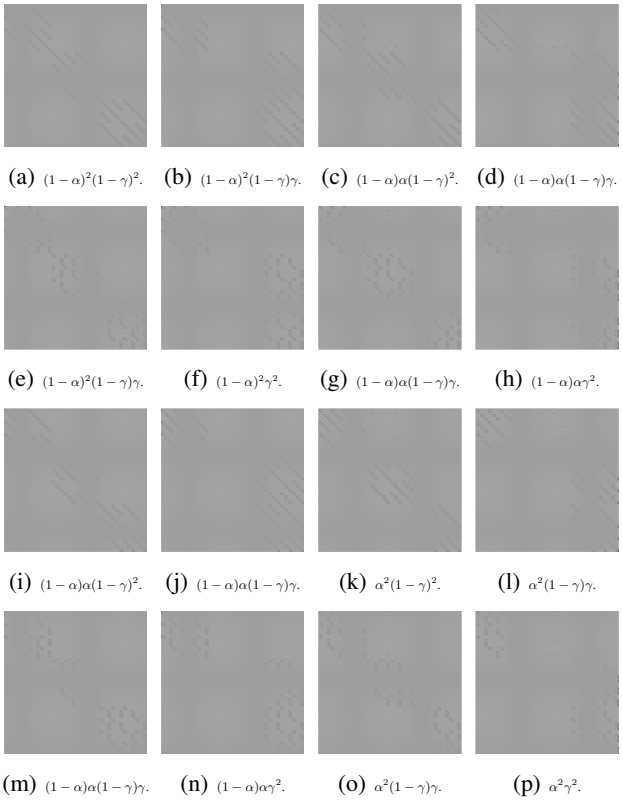

(a) $(1-\alpha)^2(1-\gamma)^2$. (b) $(1-\alpha)^2(1-\gamma)\gamma$. (c) $(1-\alpha)\alpha(1-\gamma)^2$. (d) $(1-\alpha)\alpha(1-\gamma)\gamma$.

(e) $(1-\alpha)^2(1-\gamma)\gamma$. (f) $(1-\alpha)^2\gamma^2$. (g) $(1-\alpha)\alpha(1-\gamma)\gamma$. (h) $(1-\alpha)\alpha\gamma^2$.

(i) $(1-\alpha)\alpha(1-\gamma)^2$. (j) $(1-\alpha)\alpha(1-\gamma)\gamma$. (k) $\alpha^2(1-\gamma)^2$. (l) $\alpha^2(1-\gamma)\gamma$.

(m) $(1-\alpha)\alpha(1-\gamma)\gamma$. (n) $(1-\alpha)\alpha\gamma^2$. (o) $\alpha^2(1-\gamma)\gamma$. (p) $\alpha^2\gamma^2$.

Fig. 4: Adjacency matrices of the graphs $\mathcal{G}_i$, and corresponding values of $\mu(i)$, $i = 0, \ldots, 15$.

IV. Bounds on the infection probabilities

The key advantage of using stochastic digraphs to model propagation of infectious diseases is that the computational tools developed for such a class of systems can be readily used to characterize infection probabilities.

In particular, letting $\bar{\boldsymbol{\mathcal{G}}} = (\bar{\mathcal{V}}, \bar{\boldsymbol{\mathcal{E}}}, \bar{\mu}(\cdot))$, with $\bar{\mathcal{V}} = \mathbb{Z}_{\bar{n}}$ and $\bar{\boldsymbol{\mathcal{E}}} = \{\bar{\mathcal{E}}_s\}_{s=0}^{\bar{r}-1}$, be the stochastic digraph representing the propagation of an infectious disease (which can be obtained by using Theorems 1, 3, and 2), define the set

$$\mathcal{I}_i = \Xi(\mathbb{Z}_n \times \mathbb{Z}_2 \times \cdots \times \mathbb{Z}_n \times \{1\} \times \cdots \times \mathbb{Z}_n \times \mathbb{Z}_2) \subset \mathbb{Z}_{\bar{n}},$$

where $\Xi := \sum_{i=1}^{N} (2\,n)^{i-1}(p_i + n\,s_i)$, if either $\bar{\boldsymbol{\mathcal{G}}} = \boldsymbol{\mathcal{SI}}$ or $\bar{\boldsymbol{\mathcal{G}}} = \boldsymbol{\mathcal{SIS}}$, or $\Xi := \sum_{i=1}^{N} (3\,n)^{i-1}(p_i + n\,s_i)$, if $\bar{\boldsymbol{\mathcal{G}}} = \boldsymbol{\mathcal{SIR}}$. Thus, define the following functions

$$m_i(0, \xi) := 0, \qquad \ell_i(0, \xi) := 0, \tag{5a}$$

for all $\xi \in \mathbb{Z}_{\bar{n}}$, and, for all $(k, \xi) \in \mathbb{Z}_{\geqslant 0} \times \mathbb{Z}_{\bar{n}}$,

$$m_i(k+1, \xi) := \sum_{i=0}^{\bar{r}-1} \max_{g \in Q(\xi, i)} \{\mathbb{I}_{\mathcal{I}_i}(g), m_i(k, g)\}\mu(i), \tag{5b}$$

$$\ell_i(k+1, \xi) := \sum_{i=0}^{\bar{r}-1} \min_{g \in Q(\xi, i)} \{\mathbb{I}_{\mathcal{I}_i}(g), \mathbb{I}_{\mathcal{I}_i^{\complement}} \ell_i(k, g)\}\mu(i), \tag{5c}$$

where $\mathcal{I}_i^{\complement} := \mathbb{Z}_{\bar{n}} \backslash$. The next proposition shows how the functions $m_i(k+1, \xi)$ and $\ell_i(k+1, \xi)$ can be used to bound the probability that the i-th individual become infected.

Proposition 1. *Let*

$$\xi_0 = \Xi([\ p_1(0) \quad s_1(0) \quad \cdots \quad p_N(0) \quad s_N(0)\ ]^\top).$$

Thus, for all $\kappa \in \mathbb{Z}_{\geqslant 0}$, $\kappa \geqslant 1$, $\boldsymbol{\xi} \in \mathcal{S}_r(\xi_0)$, it results

$$\ell_i(\kappa, \xi_0) \leqslant \mathbb{E}\left[\max_{k=1,\ldots,\kappa} \mathbb{I}_{\mathcal{I}_i}(\boldsymbol{\xi}_k)\right] \leqslant m_i(\kappa, \xi_0). \tag{6}$$

In particular, for all $\kappa \in \mathbb{Z}_{\geqslant 0}$, $\kappa \geqslant 1$, there exist stochastic directed paths $\underline{\boldsymbol{\xi}} \in \mathcal{S}_r(\xi_0)$ and $\overline{\boldsymbol{\xi}} \in \mathcal{S}_r(\xi_0)$ from ξ_0 such that

$$\ell_i(\kappa, \xi_0) = \mathbb{P}(\exists k \in \{1, \ldots, \kappa\} \textit{ such that } \underline{\boldsymbol{\xi}}_k \in \mathcal{I}_i), \tag{7a}$$

$$m_i(\kappa, \xi_0) = \mathbb{P}(\exists k \in \{1, \ldots, \kappa\} \textit{ such that } \overline{\boldsymbol{\xi}}_k \in \mathcal{I}_i). \tag{7b}$$

By Proposition 1, the initial condition $\xi \in \mathbb{Z}_{\bar{n}}$ of the model and the functions $\ell_i(k, \xi)$ and $m_i(k, \xi)$ can be used to establish lower and upper bounds on the probability that the i-th agent is infected at some time $\kappa \in \mathbb{Z}_{\geqslant 0}$, $\kappa \geqslant 1$, $\kappa \leqslant k$. The next example illustrates the application of Proposition 1.

Example 4. The stochastic digraphs obtained in Examples 1, 2, and 3 have been used to compute bounds on the probability that the first agent becomes infected at some time lower than or equal to k, starting at some $\xi_0 \in \mathbb{Z}_{\bar{n}}$, i.e., we computed bounds on $\mathbb{P}(\exists k \in \{1, \ldots, \kappa\}$ such that $s_k^1 = 1)$. Fig.s 5, 6, and 7 depicts the upper and lower bounds on such probability (white blocks denote probability 0, whereas black blocks denote probability 1) obtained iterating (5) and using (6), letting $\alpha = 0.75$, $\beta = 0.5$, and $\gamma = 0.1$.

We conclude this section by performing Monte Carlo simulations of the dynamical behavior of the models considered in Examples 1, 2, and 3.

Example 5. In order to validate the upper and lower bounds on the infection probability computed in Example 4, we perform Monte Carlo simulations of the behavior of the considered SI, SIS, and SIR models described in Section III. We assume that the initial state of the system is $p^1 = 0$,

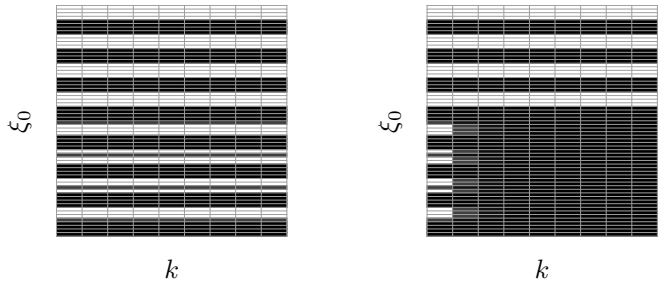

(a) Lower bound (b) Upper bound

Fig. 5: Upper and lower bounds obtained using the SI model.

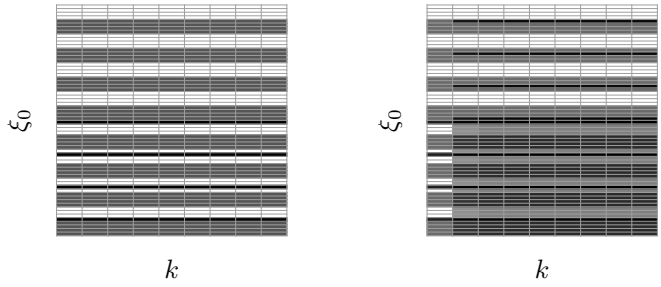

(a) Lower bound (b) Upper bound

Fig. 6: Upper and lower bounds obtained with the SIS model.

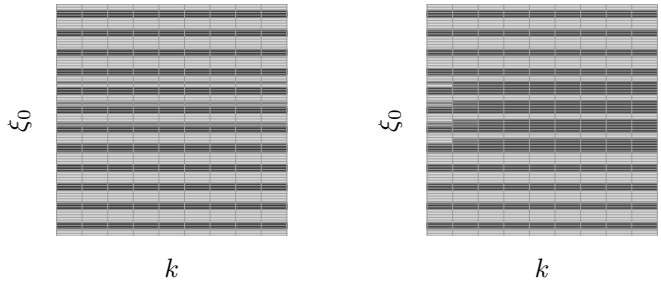

(a) Lower bound (b) Upper bound

Fig. 7: Upper and lower bounds obtained with the SIR model.

$s^1 = 0$, $p^2 = 1$, and $s^2 = 1$, i.e., at the initial time the first individual is susceptible and is in the node 0, whereas the second individual is infected and is in the node 1.

For each model, we perform 10^3 Monte Carlo simulations assuming that, at each step, the individual select the successive location uniformly at random among the ones that are in the out-neighborhood of the node corresponding to the actual position, and that the infection probabilities are the same as the one considered in Example 4. Finally, in order to approximate $\mathbb{P}(\exists k \in \{1, \dots, \kappa\}$ such that $s_k^1 = 1)$, that is the probability that the first agent is in infected status for some time lower than or equal to κ, we compute the ratio between the number of simulations in which $s_k^1 = 1$ for some $k \in \{1, \dots, \kappa\}$ and the total number of simulations.

Letting $\xi_0 = \Pi([\ p^1 \quad s^1 \quad p^2 \quad s^2\ ]^\top)$, we compare such ratios with the values of the functions $\ell_i(k, \xi_0)$ and $m_i(k, \xi_0)$ computed in Example 4. Fig. 8 depicts the obtained approximate of $\mathbb{P}(\exists k \in \{1, \dots, \kappa\}$ such that $s_k^1 = 1)$ obtained via Monte Carlo simulations and the functions $\ell_i(\kappa, \xi_0)$ and $m_i(\kappa, \xi_0)$ for $\kappa = 1, \dots, 9$, when the SI model is used.

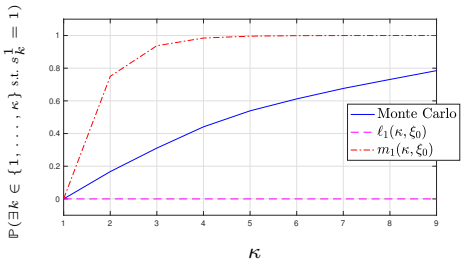

Fig. 8: Infection probabilities in the SI model.

On the other hand, Fig. 9 depicts the obtained approximate of $\mathbb{P}(\exists k \in \{1, \dots, \kappa\}$ such that $s_k^1 = 1)$ obtained via Monte Carlo simulations and the functions $\ell_i(\kappa, \xi_0)$ and $m_i(\kappa, \xi_0)$ for $\kappa = 1, \dots, 9$, when the SIS model is used.

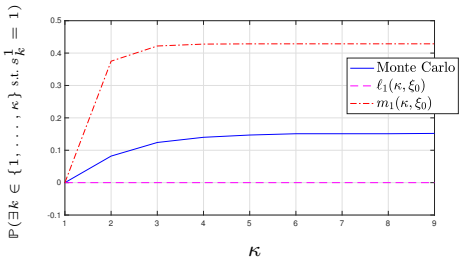

Fig. 9: Infection probabilities in the SIS model.

Finally, letting $\xi_0 = \Psi([\ p^1 \quad s^1 \quad p^2 \quad s^2\ ]^\top)$, Fig. 10 depicts the obtained approximate of $\mathbb{P}(\exists k \in \{1, \dots, \kappa\}$ such that $s_k^1 = 1)$ obtained via Monte Carlo simulations and the functions $\ell_i(\kappa, \xi_0)$ and $m_i(\kappa, \xi_0)$ for $\kappa = 1, \dots, 9$, when the SIR model is used.

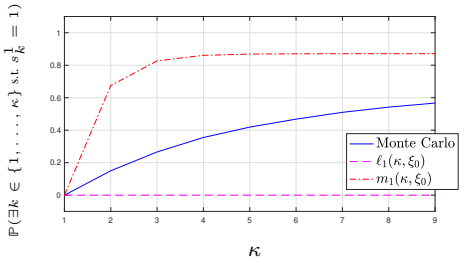

Fig. 10: Infection probabilities in the SIR model.

As shown by Fig.s 8, 9, and 10, in all the considered cases, $\ell_1(\kappa, \xi_0) \leqslant \mathbb{P}(\exists k \in \{1, \dots, \kappa\}$ such that $s_k^1 = 1) \leqslant m_1(\kappa, \xi_0)$ for all $\kappa \in \{1, \dots, 9\}$, thus confirming the theoretical results given in Proposition 1. Furthermore, there exist stochastic directed paths $\underline{\boldsymbol{\xi}} \in \mathcal{S}_r(\xi_0)$ and $\overline{\boldsymbol{\xi}} \in \mathcal{S}_r(\xi_0)$ such that (7) holds. Thus, there exist stochastic directed paths such that $\mathbb{P}(\exists k \in \{1, \dots, \kappa\}$ s.t. $s_k^1 = 1) = 0$, i.e., the first agent is not infected almost surely for all $k \in \{1, \dots, \kappa\}$. This is essentially due to the fact that individuals are allowed

to move so that the first agent does not share the same position of an infected individual at any step $k \in \{1, \dots, \kappa\}$. Such a behavior can be prevented by suitably redefining the digraph of the admissible motions (shown in Fig. 1).

V. Conclusions

In this paper, we present a framework for modeling epidemic spreading in populations of mobile agents, using stochastic digraphs. The key advantage of using this mathematical framework is that all the tools available for such a class of systems can be readily and efficiently used to quantitatively characterize the properties of the epidemic diffusion. In particular, the preliminary results here reported show that simple computational tools can be employed to determine bounds on the probability that a certain individual is infected, given the initial condition of all the other individuals.

Future work will deal with the extension of the obtained results to more general classes of infectious diseases [30], with providing further computational tools to characterize the probabilistic behavior of the propagation of the disease, and with designing pinning control strategies to limit the spread of the infection [31], thus allowing to plan optimal vaccination strategies. In particular, one of the objectives of our future research is to adapt the Lyapunov-like tools given in [23] to characterize local asymptotic stability, local recurrence, and local reachability in probability of some states in the stochastic digraph. This will allow us to determine critical thresholds for the propagation of the disease and to determine the sensitivity to changes in parameter values.

A critical issue of the presented approach is that the number of nodes of the digraphs modeling the diffusion of infectious diseases grows exponentially with the size of the population, thus rapidly increasing the computational burden. A further objective of our future research is to use sparsity features and approximate dynamic programming tools [32] to determine the bounds used in Proposition 1.

Acknowledgements

A.R. acknowledges financial support from Compagnia di San Paolo and from the Italian Ministry of Foreign Affairs and International Cooperation, within the project "Mac2Mic", Macro to Micro: uncovering the hidden mechanisms driving network dynamics, in the framework of the bilateral agreement Italy/Israel.

References

[1] H. W. Hethcote, "The mathematics of infectious diseases," *SIAM review*, vol. 42, no. 4, pp. 599–653, 2000.

[2] C. Nowzari, V. M. Preciado, and G. J. Pappas, "Analysis and control of epidemics: A survey of spreading processes on complex networks," *IEEE Control Systems Magazine*, vol. 36, no. 1, pp. 26–46, 2016.

[3] W. O. Kermack and A. G. McKendrick, "A contribution to the mathematical theory of epidemics," *Proceedings of the royal society of london. Series A*, vol. 115, no. 772, pp. 700–721, 1927.

[4] N. T. J. Bailey, *The mathematical theory of infectious diseases and its applications*. Charles Griffin & Company, 1975.

[5] R. M. Anderson, *The population dynamics of infectious diseases: theory and applications*. Springer, 2013.

[6] N. J. Watkins, C. Nowzari, and G. J. Pappas, "A robust moment closure for general continuous-time epidemic processes," in *IEEE Conference on Decision and Control*, pp. 244–249, 2018.

[7] R. M. Anderson and R. M. May, *Infectious diseases of humans: dynamics and control*. Oxford university press, 1992.

[8] O. Diekmann, H. Heesterbeek, and T. Britton, *Mathematical tools for understanding infectious disease dynamics*, vol. 7. Princeton University Press, 2012.

[9] A. Lajmanovich and J. A. Yorke, "A deterministic model for gonorrhea in a nonhomogeneous population," *Mathematical Biosciences*, vol. 28, no. 3-4, pp. 221–236, 1976.

[10] Y. Wang, D. Chakrabarti, C. Wang, and C. Faloutsos, "Epidemic spreading in real networks: An eigenvalue viewpoint," in *22nd International Symposium on Reliable Distributed Systems*, pp. 25–34, IEEE, 2003.

[11] P. Van Mieghem, "The n-intertwined SIS epidemic network model," *Computing*, vol. 93, no. 2-4, pp. 147–169, 2011.

[12] W. Mei and F. Bullo, "Modeling and analysis of competitive propagation with social conversion," in *53rd IEEE Conference on Decision and Control*, pp. 6203–6208, 2014.

[13] N. Perra, B. Gonçalves, R. Pastor-Satorras, and A. Vespignani, "Activity driven modeling of time varying networks," *Scientific reports*, vol. 2, p. 469, 2012.

[14] A. Rizzo, M. Frasca, and M. Porfiri, "Effect of individual behavior on epidemic spreading in activity-driven networks," *Physical Review E*, vol. 90, no. 4, p. 042801, 2014.

[15] M. Starnini and R. Pastor-Satorras, "Temporal percolation in activity-driven networks," *Physical Review E*, vol. 89, no. 3, p. 032807, 2014.

[16] Y. Zou, W. Deng, W. Li, and X. Cai, "A study of epidemic spreading on activity-driven networks," *International Journal of Modern Physics C*, vol. 27, no. 08, p. 1650090, 2016.

[17] P. E. Paré, C. L. Beck, and A. Nedić, "Epidemic processes over time-varying networks," *IEEE Transactions on Control of Network Systems*, vol. 5, no. 3, pp. 1322–1334, 2018.

[18] M. Frasca, A. Buscarino, A. Rizzo, L. Fortuna, and S. Boccaletti, "Dynamical network model of infective mobile agents," *Physical Review E*, vol. 74, no. 3, p. 036110, 2006.

[19] M. Coffee, M. N. Lurie, and G. P. Garnett, "Modelling the impact of migration on the HIV epidemic in south africa," *Aids*, vol. 21, no. 3, pp. 343–350, 2007.

[20] Y. Muroya, Y. Enatsu, and T. Kuniya, "Global stability of extended multi-group SIR epidemic models with patches through migration and cross patch infection," *Acta Mathematica Scientia*, vol. 33, no. 2, pp. 341–361, 2013.

[21] K. Hadeler, "The role of migration and contact distributions in epidemic spread," in *Bioterrorism: Mathematical Modeling Applications in Homeland Security*, pp. 199–210, SIAM, 2003.

[22] S. Castles, H. De Haas, and M. J. Miller, *The age of migration: International population movements in the modern world*. Macmillan International Higher Education, 2013.

[23] C. Possieri and A. R. Teel, "Weak reachability and strong recurrence for stochastic directed graphs in terms of auxiliary functions," in *55th Conference on Decision and Control*, pp. 3714–3719, IEEE, 2016.

[24] C. Possieri and A. R. Teel, "Asymptotic stability in probability for stochastic Boolean networks," *Automatica*, vol. 83, pp. 1–9, 2017.

[25] B. Bollobás, *Modern Graph Theory*. Springer New York, 1998.

[26] R. Diestel, *Graph Theory*. Springer Verlag, 2006.

[27] A. Subbaraman and A. R. Teel, "A converse Lyapunov theorem for strong global recurrence," *Automatica*, vol. 49, no. 10, pp. 2963–2974, 2013.

[28] S. Grammatico, A. Subbaraman, and A. R. Teel, "Discrete-time stochastic control systems: examples of robustness to strictly causal perturbations," in *52nd Conference on Decision and Control*, pp. 6403–6408, IEEE, 2013.

[29] A. R. Teel, J. P. Hespanha, and A. Subbaraman, "A converse Lyapunov theorem and robustness for asymptotic stability in probability," *IEEE Transactions on Automatic Control*, vol. 59, no. 9, pp. 2426–2441, 2014.

[30] L. Zino, A. Rizzo, and M. Porfiri, "An analytical framework for the study of epidemic models on activity driven networks," *Journal of Complex Networks*, vol. 5, no. 6, pp. 924–952, 2017.

[31] X. F. Wang and G. Chen, "Pinning control of scale-free dynamical networks," *Physica A: Statistical Mechanics and its Applications*, vol. 310, no. 3-4, pp. 521–531, 2002.

[32] W. B. Powell, *Approximate Dynamic Programming: Solving the curses of dimensionality*. John Wiley & Sons, 2007.